Journal of Applied Sciences

ISSN 1812-5654

science alert

ANSInet
an open access publisher
http://ansinet.com

Journal of Applied Sciences 8 (14): 2544-2552, 2008
ISSN 1812-5654

Analysis of Natural Convection in Liquid Nitrogen under Storage Conditions

M. Belmedani, A. Belgacem and R. Rebiai
Département de Génie Chimique et de Cryogénie, Faculté de Génie Mécanique et Génie des Procédés,
U.S.T.H.B., B.P. No. 32 El Alia Bab Ezzouar Alger 16111

Abstract: This study discusses the behaviour of convective heat transfer at low temperature storage tank containing non boiling liquid nitrogen. The aim of this experimental and theoretical study is to have a better understanding of the instability phenomena occurring in cryogenic liquids under storage conditions. The thermodynamic model we developed in this study, describing both the Interfacial thermal boundary layer and the wall boundary layer, is based on the experimental data at the laboratory scale. Experimental study gives a better indication on the evaporation mechanism of the stored liquid near the evaporative surface region. The temperature difference between the surface and the bulk liquid for various absorptive heat flows resulting in different rate of evaporation was measured for a cryogenic liquid stored. Theoretical study devoted to the free convection theory by using the integral approach including the coupling of dynamic and thermal phenomena gives the temperature and velocity profiles in laminar and turbulent wall boundary layers at various wall heat flux as well as the evolution of the thickness of the interfacial boundary layer as a function of the evaporated mass flow.

Key words: Liquid nitrogen, natural convection, modelling, boundary layer, storage

INTRODUCTION

Nowadays, the cryogenic techniques are currently applied in different energy fields such as hydrocarbons and gas industries (liquefaction, gas separation, storage, transportation), agro-alimentary, biomedical, iron and steel industry. These low and very low temperatures techniques are obtained using the cryogenic liquids such as nitrogen (LIN:-196°C), hydrogen (LH_2:-253°C), oxygen (LOX:-183°C), argon (LAr:-187°C), liquefied natural gas (LNG:-161°C) and helium (LHe:-269°C).

In Algeria, the application of cryogenic technology remains dominated by different processes of liquefaction (Cascade, APCI, PRICO), storage and transportation of liquefied natural gas and derivative (LNG, LPG, LHe) with a total liquefaction capacity of about 40 billions m^3. Once liquefied, LNG is then stored in a special above ground tanks reaching up to 100,000 m^3 storage capacity each.

Although the storage tanks are made of 9% nickel steel to sustain low temperature and resist to the thermal shocks and well isolated with perlite, they inevitably conduct heat of the surroundings towards the liquid bulk along the inner wall, the tank floor instrumentation cables, transfer pipes and even the isolated space. The amount of heat entering the liquid bulk is carried upwards by convection currents to the surface where evaporation takes place. The excess heat which not released by surface evaporation returns to the liquid core where a secondary convection currents produces mixing.

Hazardous variations in the evaporation rate, normal boil-off, seems to be a major concern of the storage behaviour of liquefied gases such as LNG, LPG, LIN, LOX, LH2, LHe, LAr, … These variations in the boil-off during the normal storage conditions of cryogenic liquids, which can be reproduced in small containers at the laboratory level (miniature vapour explosion), should not be tolerated in industrial scale liquid storage tank. Although the phenomena was clearly observed and reported by Rebiai *et al.* (1984), the mechanisms of the evaporative liquid surface, leading to these phenomena are not fully understood.

Within this framework and in the hope of making contribution to a better comprehension and the explanation of these phenomena of instability related to the degrees of stratification and overheating, we undertook an experimental and theoretical studies relating to the temperature distribution according to the rate of evaporation.

This study discuss the behaviour of the heat transfer within the interfacial thermal boundary layer as well as in that developed on the side wall of a storage tank of cryogenic liquid when a density flux is imposed.

Corresponding Author: Belmedani Mohamed, Département de Génie Chimique et de Cryogénie,
Faculté de Génie Mécanique et Génie des Procédés, U.S.T.H.B.,
B.P. No. 32 El Alia Bab Ezzouar Alger 16111 Tel: 00 213 21 24 79 19 Fax: 00 213 21 24 79 19

Several studies were undertaken in the field of the natural convection in enclosures: Evans *et al.* (1968) carried out experimental studies of heat transfer in liquids contained in vertical and horizontal enclosures. Excellent bibliographical reviews concerning the laminar natural convection in enclosures were published by Ostrach (1988) and Catton (1978). Kadja and Hacene (1999) presented digital simulations of the natural convection of a liquid subjected to variable parietal conditions. Khemis *et al.* (2003, 2004) and Boukeffa *et al.* (2001) presented measurements and numerical analysis of the heat transfers coupled in a cryogenic tank. Papanicolaou and Belessiotis (2001) studied numerically the transient state of natural convection in a vertical cylindrical enclosure at high Rayleigh numbers where several two-equation turbulence models are used. De Lorenzo (2002) presented an investigation on laminar transient free convection along vertical surface subjected to a periodical heat flux density. Khelifi Touhami *et al.* (2005) treated laminar natural convection in cylindrical enclosure in LNG storage tank used finite differences numerical method. Belmedani *et al.* (2007) determines numerically and analyses the dynamic and thermal fields resulting from natural convection in LNG tank. Rashed and Kassem (2007) discuss the steady laminar natural convection in vertical plate of a fluid having chemical reaction.

MATERIALS AND METHODS

The cryostat has been initially developed by Rebiai (1985) and later improved by Belmedani (1994) is a cylindrical double-walled tank silvered Pyrex flask. Temperature measurements were obtained using a specially made differential micro-thermocouple with fast response time realised with very fine wires (25 μm diameter) of copper and constantan. The micro-thermocouple was previously calibrated against a platinum resistance thermometer.

The evaporation rate from the inner Dewar, having 80 mm inner diameter, was varied using a specially made uniform heat flux electrical heater mounted in the vacuum space around the inner wall of the inner Dewar. The outer cryostat was filled with liquid nitrogen as a shield to absorb heat from the surrounding so that the only heat transferred to the liquid under analysis is from the electrical heater which can be monitored accordingly.

Measurements were taken at the centre, near the walls and at different levels in the bulk liquid.

To avoid nucleation problems, each of the liquid samples was filtered using either a sintered glass micro-filter (5-15 μm pore sizes) or cotton wool. The measurements were recorded once the thermal equilibrium was attained.

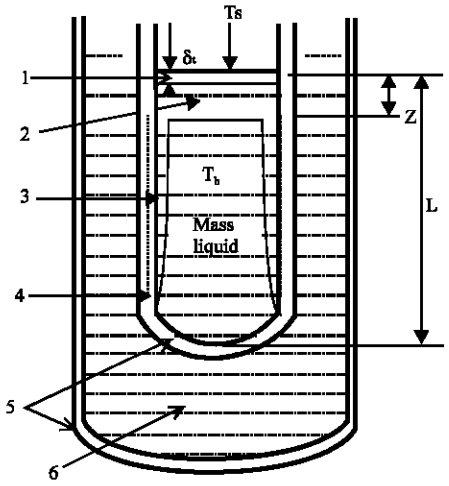

Fig. 1: Natural convection in liquid nitrogen cryostat with constant wall heat flux (1) thermal boundary layer, (2) mixture region, (3) parietal boundary layer, (4) electrical resistance, (5) vacuum space and (6) coolant

The data points were recorded using a computer controlled data logger by fixing the main junction below the surface of the liquid and allowing the liquid level to fall by evaporation which required several minutes of waiting, depending on the heat input.

The evaporation rate was recorded for each run by direct reading of the Hastings gas flow meter.

Modelling: Based on the observations and experimental analysis as well as the results established by Rebiai (1985) and Belmedani (1994) and for obvious experimental reasons and in regard to the difficulties and contradictions met for the validation of the models, boundary layers approach was used. A thermodynamic model developed by Evans *et al.* (1968) was selected and adopted in our case. However, taking into account evaporation to the interface (Fig. 1).

The modelling of the problem requires the following simplifying assumptions:

- The temperatures of the surface Ts and that of the liquid bulk Tb are uniform and homogeneous apart from the boundary layer region
- The absence of vertical gradients in temperature along the walls in the interfacial boundary layer
- The contribution of heat transfer by radiation and vapour can be neglected
- The thicknesses of the boundary layers at the walls and the interface, are negligible compared to the dimensions of the cryostat

- The velocity of evaporation in the stable condition is identical in each point of surface

Interfacial thermal boundary layer: The assessment of the heat flux in this boundary layer can be written at first approximation like:

$$\varphi_F + \varphi_L = \dot{m} L_v \quad (1)$$

Expression in which all the heat transferred by conduction through the layer thickness δ_L towards the interface is used for the reaction of evaporation:

$$\varphi_F + \varphi_L = \frac{k_L (T_b - T_S)}{\delta_L} \quad (2)$$

With $\delta_L = k_L/h$, thickness of conductive film crossed by energy arriving at the interface by convection. Where h is the coefficient of heat transfer in the area subjacent with the interface.

In addition, the interfacial thermal thickness of boundary layer δ_t is given by Taine and Petit (1989):

$$\delta_t = \frac{3}{2}\frac{k_L}{h} \quad (3)$$

Then, the interfacial thermal thickness of boundary layer δ_t according to δ_L is:

$$\delta_t = \frac{3}{2}\delta_L \quad (4)$$

That is to say:

$$\delta_t = \frac{3k_L (T_b - T_S)}{2\dot{m} L_v} \quad (5)$$

The experimental study highlights a dependence of the variations of the mass flow evaporated m according to the degree of overheating ($\Delta T = T_b - T_s$) as shown in the Fig. 2 whose approximation is given in the case of liquid nitrogen (LIN) by:

$$\dot{m} = 3.38\ 10^{-3}\ \Delta T^{1.18} \quad (6)$$

The vertical temperature profile at different liquid levels, was found to be in qualitative agreement with theoretical models according to the molecular theory of evaporation. Figure 3 shows the evolution of the thickness of the interfacial thermal boundary layer according to the evaporated mass flow calculated by the approximations used on the preceding figure.

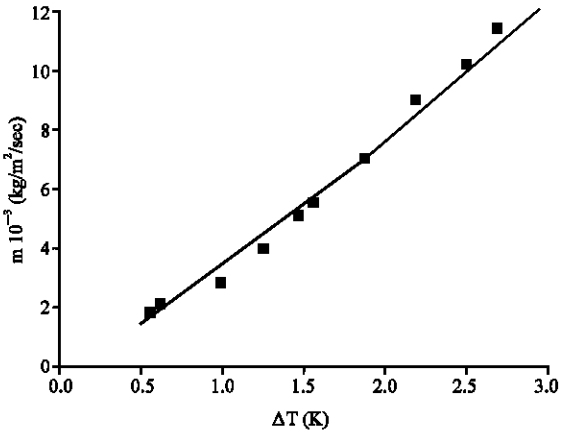

Fig. 2: The variations of the evaporated mass flow according to the degree of overheating

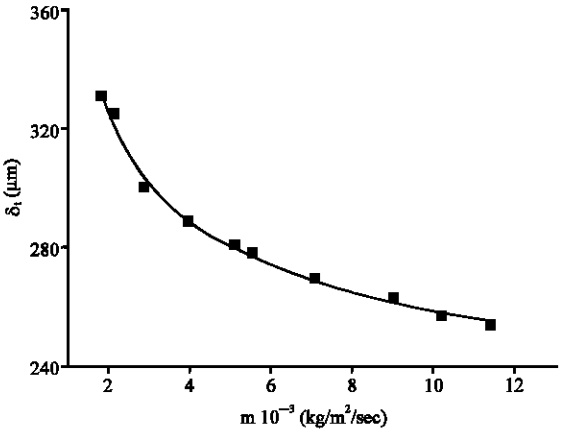

Fig. 3: Evolution of the thickness of the interfacial boundary layer with the evaporated mass flow

The Rayleigh number which governs the stability of the stationary conductive state of the interfacial thermal boundary layer is defined by:

$$Ra = \frac{g\beta(T_b - T_s)\delta_t^3}{\alpha\upsilon} \quad (7)$$

The variation of Rayleigh number, starting from the Eq. 7 of the experimental values (T_b-T_s) and the computed values of δ_t, is given in the Fig. 4.

The number of Rayleigh in the interfacial thermal boundary layer increases with the mass flow evaporated m, but remains lower than critical Rayleigh (Rac = 657.5, Chandrasekhar, 1962).

Wall boundary layer: The thickness of wall boundary layer being small compared to the rayon of the cryostat, the heat transfer from the wall of cryostat is the same as that from a vertical plate.

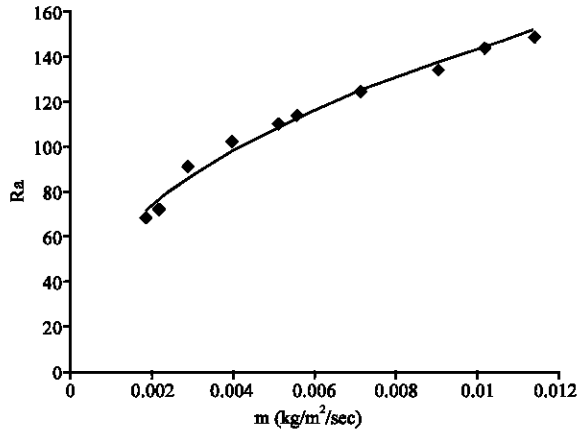

Fig. 4: Evolution of the Rayleigh number with the evaporated mass flow in interfacial boundary layer

The system of equations governing the convective boundary layers for natural convection in the storage tank is (Incropera and Dwitt, 2002; Polidori *et al*., 2003):

Continuity equation $$\frac{\partial u}{\partial x}+\frac{\partial v}{\partial y}=0 \quad (8)$$

Momentum equation $$u\frac{\partial u}{\partial x}+v\frac{\partial u}{\partial y}=g\beta(T-T_\infty)+\frac{1}{\rho}\frac{\partial \tau_{yx}}{\partial y} \quad (9)$$

Energy equation $$u\frac{\partial T}{\partial x}+v\frac{\partial T}{\partial y}=\alpha\frac{\partial^2 T}{\partial y^2} \quad (10)$$

This system is very complex and generally requires simplifications to solve it.

By multiplying the Eq. 8 by the velocity, u and by adding the first member of the equation obtained to the Eq. 9 we will obtain

$$\frac{\partial u^2}{\partial x}+\frac{\partial (u.v)}{\partial y}=g\beta(T-T_\infty)+\frac{1}{\rho}\frac{\partial \tau_{yx}}{\partial y} \quad (11)$$

The integration of Eq. 11 in relation to y gives:

$$\int_0^\delta \frac{\partial u^2}{\partial x}dy+\int_0^\delta \frac{\partial (u.v)}{\partial y}dy=g.\beta\int_0^\delta (T-T_\infty)dy+\frac{1}{\rho}\int_0^\delta \frac{\partial \tau_{yx}}{\partial y}dy \quad (12)$$

from where

$$\frac{\partial}{\partial x}\int_0^\delta u^2dy=\left[(u.v)(\delta)-(u.v)(0)\right]+ g\beta\int_0^\delta (T-T_\infty)dy+\frac{1}{\rho}\left[\tau_{yx}(\delta)-\tau_{yx}(0)\right] \quad (13)$$

Boundary conditions, which apply to problem (at the wall and at the border of the boundary layer) are

$$u(0)=v(0)=0,\quad u(\delta)=v(\delta)=0 \quad (14a)$$

$$\tau_{yx}(0)=\tau_P,\quad \tau_{yx}(\delta)=0 \quad (14b)$$

Taking into account the Eq. 14a and 14b, the momentum equation becomes

$$\frac{\partial}{\partial x}\int_0^\delta u^2dy=g\beta\int_0^\delta (T-T_\infty)dy-\frac{1}{\rho}.\tau_p \quad (15)$$

By multiplying the Eq. 8 by the temperature T and by adding the first member of the equation obtained with the Eq. 10 we will have

$$\frac{\partial (u.T)}{\partial x}+\frac{\partial (v.T)}{\partial y}=\alpha\frac{\partial^2 T}{\partial y^2} \quad (16)$$

The integration of the this equation gives

$$\int_0^\delta \frac{\partial (u.T)}{\partial x}dy+\int_0^\delta \frac{\partial (v.T)}{\partial y}dy=\alpha\int_0^\delta \frac{\partial^2 T}{\partial y^2}dy \quad (17)$$

From where

$$\frac{\partial}{\partial x}\int_0^\delta (u.T)dy+\left[(v.T)(\delta)-(v.T)(0)\right]=\alpha\left[\frac{\partial T}{\partial y}(\delta)-\frac{\partial T}{\partial y}(0)\right] \quad (18)$$

On the wall and the border of the boundary layer, boundary conditions applied to problem are

$$T(0)=T_p,\ v(0)=0,\quad T(\delta)=T_\infty,\ v(\delta)=0 \quad (19a)$$

$$\frac{\partial T}{\partial y}(\delta)=0,\quad \frac{\partial T}{\partial y}(0)=-\frac{\alpha.\varphi_p}{\rho.c_p} \quad (19b)$$

Taking into account the Eq. 19a and b, Eq. 18 becomes

$$\frac{\partial}{\partial x}\int_0^\delta u.Tdy=\frac{\varphi_p}{\rho.c_p} \quad (20)$$

While adding

$$-\int_0^\delta u\frac{\partial T_\infty}{\partial x}dy$$

to the two members of the Eq. 20, one leads to

$$\frac{\partial}{\partial x}\int_0^\delta u(T-T_\infty)dy=\frac{\varphi_p}{\rho.c_p}-\int_0^\delta u\frac{\partial T_\infty}{\partial x} \quad (21)$$

In natural convection the temperature into free current (free stream) T_∞ is constant.

From where $$\frac{\partial T_\infty}{\partial x} = 0 \quad (22)$$

Finally, the integral forms of the momentum and energy equations in natural convection in steady flow are

$$\frac{\partial}{\partial x}\int_0^\delta u^2 dy = g\beta\int_0^\delta (T - T_\infty)\, dy - \frac{1}{\rho}.\tau_p \quad (23)$$

$$\frac{\partial}{\partial x}\int_0^\delta u(T - T_\infty) dy = \frac{\varphi_p}{\rho.c_p} \quad (24)$$

The velocity, u, is driven by buoyancy, which is reflected in the term $g\beta(T-T_\infty)$ in the momentum equation. The density, ρ, varies with temperature T, so it is impossible to solve the momentum and energy equations independently of one another.

In natural convection, the velocity and temperature profiles commonly adopted within the corresponding boundary layers are expressed in the form of the power laws of the type (Eckert and Jackson, 1950).

In laminar natural convection

$$u = \omega\frac{y}{\delta}(1 - \frac{y}{\delta})^2 \quad (25)$$

$$T - T_\infty = \frac{\varphi_P}{2k}\delta(1 - \frac{y}{\delta})^2 \quad (26)$$

In turbulent natural convection

$$u = \omega\left(\frac{y}{\delta}\right)^{\frac{1}{7}}\left(1 - \frac{y}{\delta}\right)^4 \quad (27)$$

$$T - T_\infty = \left(T_p - T_\infty\right)\left[1 - \left(\frac{y}{\delta}\right)^{\frac{1}{7}}\right] \quad (28)$$

In laminar natural convection and after carrying forward the various profiles Eq. 25 and 26 and application of the wall shear stress $\tau_P = -\mu\frac{\partial u}{\partial y}\Big|_{y=0}$ the analytical resolution of the system of the momentum and energy equations by using non dimensional variables (Belmedani, 1994), the variables of origin ω and δ will be connected to position x and heat flux φ_P by:

$$\delta(x) = \frac{C_1^{\frac{2}{3}}}{C_2^{\frac{1}{3}}(\frac{g\alpha}{k\upsilon^2})^{\frac{1}{5}}}(\frac{x}{\varphi_p})^{\frac{1}{5}} \quad (29)$$

$$\omega(x) = (\frac{g\alpha\upsilon^{\frac{1}{2}}}{k})^{\frac{2}{5}}\frac{C_2^{\frac{2}{3}}}{C_1}\varphi_P^{\frac{2}{5}}x^{\frac{3}{5}} \quad (30)$$

With

$$C_1 = \frac{60}{Pr}$$

and

$$C_2 = C_1^{\frac{4}{5}}(\frac{10}{0.2 + Pr})^{\frac{3}{5}}$$

In the case of the liquid nitrogen whose physical properties are given by Lienhard and Lienhardal (2005). These expressions are written by:

$$\delta(x) = 7.47610^{-3}(\frac{x}{\varphi_P})^{\frac{1}{5}} \quad (31)$$

$$\omega(x) = 10.7910^{-3}\varphi_P^{\frac{2}{5}}x^{\frac{3}{5}} \quad (32)$$

Figure 5 and 6 give the velocity and temperature profiles for liquid nitrogen in the laminar boundary layer at x = 0.15 m for both wall heat flux (300 and 500 W m^{-2}). It can be seen that in the laminar mode the velocity profile increases gradually and the temperature profile decreases gradually according to horizontal position.

In turbulent natural convection, the closure problem can be carried out by application of the analogy of Reynolds who establishes a correlation between the density of flow and the wall shear stress:

$$\frac{\varphi_p}{\tau_p.c_p} = \frac{T_P - T_\infty}{u_\infty} \quad (33)$$

While taking, like empirical expression of the wall shear stress, that derive from the convection forced in control, Kakaç and Yener (1995) extended to the natural convection:

$$\tau_p = 0.0225.\omega^2.\rho.\left(\frac{\upsilon}{\omega\delta}\right)^{\left(\frac{1}{4}\right)} \quad (34)$$

Equation can be combined with known velocity profile at border of the boundary layer and substituted in Eq. 33, we find

$$T_p - T_\infty = \frac{\varphi_p.\omega^{-\frac{3}{4}}.\delta^{\frac{1}{4}}}{0.0225.\rho.\upsilon^{0.25}.c_p} \quad (35)$$

The substitution of the Eq. 35 in Eq. 28 gives

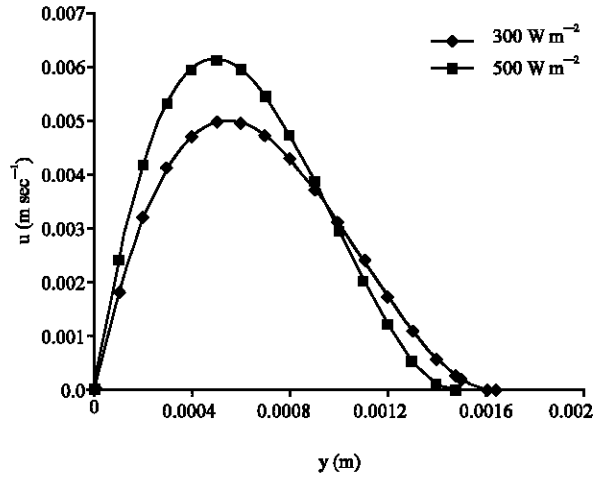

Fig. 5: Velocity Profile in wall laminar boundary layer for liquid nitrogen at different wall heat flux (x = 0.15 m)

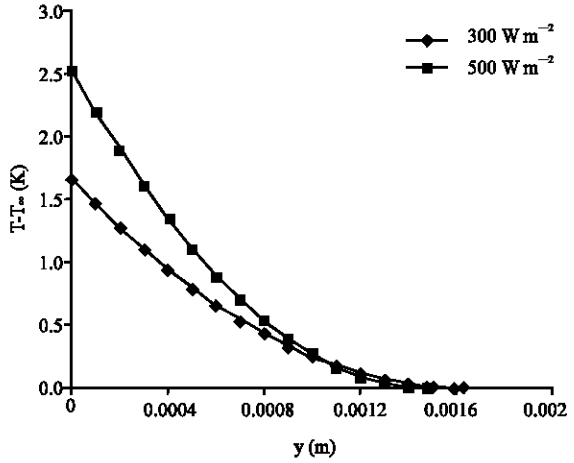

Fig. 6: Temperature profile in wall laminar boundary layer for liquid nitrogen at different wall heat flux (x = 0.15 m)

$$T - T_\infty = \frac{\varphi_p.\omega^{-\frac{3}{4}}.\delta^{\frac{1}{4}}}{0.0225.\rho.\upsilon^{0.25}.c_p}\left[1-\left(\frac{y}{\delta}\right)^{\frac{1}{7}}\right] \quad (36)$$

Let us replace the Eq. 28, 35 and 36 in the integral form of the momentum equation, we get

$$\frac{\partial}{\partial x}\int_0^\delta \omega^2\left(\frac{y}{\delta}\right)^{\frac{2}{7}}\left(1-\frac{y}{\delta}\right)^8 dy = g\beta\int_0^\delta \frac{\varphi_p.\omega^{-\frac{3}{4}}.\delta^{\frac{1}{4}}}{0.0225.\rho.\upsilon^{0.25}.c_p}\left[1-\left(\frac{y}{\delta}\right)^{\frac{1}{7}}\right]dy - 0.0225\omega^2\left(\frac{\upsilon}{\omega\delta}\right)^{\frac{1}{4}} \quad (37)$$

If we put $z = y/\delta$, $dy = \delta.dz$ and replace the Eq. 28 and 35 in the integral form of the equation of energy, we obtain

$$\frac{\varphi_p}{\rho.c_p} = \frac{\partial}{\partial x}\int_0^1 \omega\delta.z^{\frac{1}{7}}(1-z)^4\left(1-z^{\frac{1}{7}}\right)\frac{\varphi_p.\omega^{-\frac{3}{4}}.\delta^{\frac{1}{4}}}{0.0225.\rho.\upsilon^{0.25}.c_p}dz \quad (38)$$

From where

$$\frac{\partial}{\partial x}\left[\omega^{\frac{1}{4}}.\delta^{\frac{5}{4}}\right] = 0.61425.\upsilon^{\frac{1}{4}} \quad (39)$$

Now we put

$$\omega = C_1.x^n \qquad \delta = C_2.x^m \quad (40)$$

The resolution of this system of equation gives

$$n = \frac{3}{7},\ m = \frac{5}{7} \quad (41)$$

After we found the powers of x in $\omega(x)$ and $\delta(x)$, the constants C_1 and C_2 should be calculated with the values of n and m found, which gives

$$\frac{11}{7}C_1^2.C_2 = 106.2\frac{g.\beta.\varphi_p}{\rho.\upsilon^{\frac{1}{4}}.c_p}C_1^{-\frac{3}{4}}.C_2^{\frac{5}{4}} - 0.43\,\upsilon^{0.25}.C_1^{\frac{7}{4}}.C_2^{-\frac{1}{4}} \quad (42)$$

$$0.6143.\upsilon^{0.25} = C_1^{\frac{1}{4}}.C_2^{\frac{5}{4}} \quad (43)$$

With the preceding equations, we obtain the relation which relate C_1 to C_2

$$C_1 = \frac{0.1424\,\upsilon}{C_2^5} \quad (44)$$

By replacing the Eq. 44 in the Eq. 42 we will have

$$C_2 = \left[\frac{\rho.\upsilon^3.c_p}{9808.18.g.\beta.\varphi_p}\right]^{\frac{1}{14}} = \left[\frac{k.Pr.\upsilon^2}{9808.18.g.\beta.\varphi_p}\right]^{\frac{1}{14}} \quad (45)$$

Let us replace the expression of C_2 in the Eq. 42-44, we obtain:

$$C_1 = \frac{3.7965\,\upsilon}{\left[\frac{k.Pr.\upsilon^2}{g.\beta.\varphi_p}\right]^{\frac{5}{14}}} \quad (46)$$

By replacing the expressions 42 and 46 in the system of Eq. 40 we obtain finally

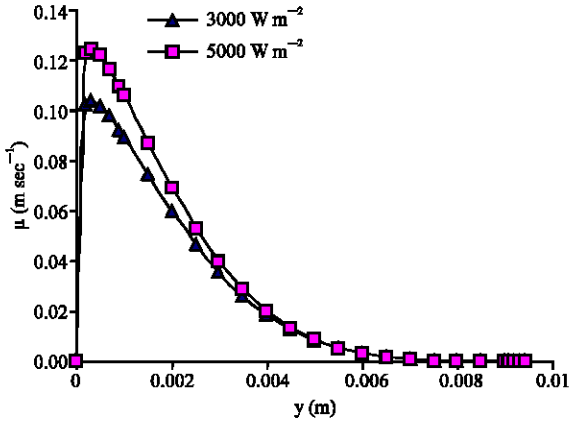

Fig. 7: Velocity profile in turbulent wall boundary layer for liquid nitrogen at different wall heat flux (x = 0.15 m)

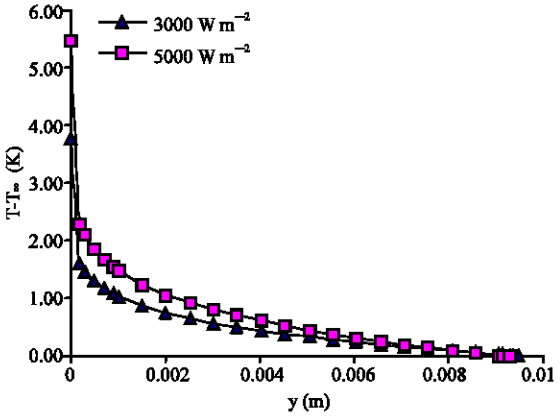

Fig. 8: Temperature profile in wall turbulent boundary layer for liquid nitrogen at different wall heat flux (x = 0.15 m)

$$\omega = \frac{3.7965.\upsilon}{\left[\frac{k.Pr.\upsilon^2}{g.\beta.\varphi_p}\right]^{\frac{5}{14}}}.x^{\frac{3}{7}} \quad (47)$$

$$\delta = 0.5187\left[\frac{k.Pr.\upsilon^2}{g.\beta.\varphi_p}\right]^{\frac{1}{14}}.x^{\frac{5}{7}} \quad (48)$$

The physical properties of liquid nitrogen are those used by Lienhard and Lienhard (2005). These expressions become:

$$\delta(x) = 6.52\ \ 10^{-2}\left(\frac{1}{\varphi_P}\right)^{\frac{1}{14}}x^{5/7} \quad (49)$$

$$\omega(x) = 2.443\ 10^{-2}\ \varphi_P^{\frac{5}{14}}\ x^{\frac{3}{7}} \quad (50)$$

The substitution of Eq. 49 and 50 in 35, 36 and 27, permit us to plot the velocity and temperature profiles (Fig. 7, 8) for liquid nitrogen in wall boundary layer at x = 0.15 m for both wall heat flux (3000 and 5000 W m^{-2}). It can be seen that in the turbulent mode the velocity profile increases abruptly near to the wall whereas the temperature profile falls abruptly near to the wall according to the horizontal position.

DISCUSSION

Although many studies related to the turbulent natural convection along an isothermal vertical wall can be found in the literary, the case of a uniformly heated vertical surface was treated much less in spite of its interest.

In the interfacial thermal boundary layer, the Rayleigh number increases with the mass flow evaporated m, but remain lower than critical Rayleigh.

Indeed the experiments show that a conducting boundary layer and without movement exists with the lower part of the interface, where the convective phenomenon which relates to the volume of the liquid does not interact directly with the evaporative phenomenon, which is localised on the free face.

According to the results obtained in parietal boundary layer, we note that the thickness of dynamic and thermal boundary layer increase with the vertical position and decrease with the heat flow. On the other hand, the maximum velocity increases with the heat flow and the vertical position. The maximum value of velocity in the turbulent mode is larger than that of the laminar mode.

This difference in behaviour in the two modes can be explained by the thermal energy conversion into kinetic energy and this transformation is larger in the turbulent mode on account of the characteristics of this last.

The reduction in the wall boundary layer with the heat flow (difference in temperature) can be explained by the increase in the rates of mixture and diffusivity because of the increases in convective currents. These currents supply unceasingly from thermal energy brought by the heat flow what reduces the thickness of boundary layer because thermal energy is transformed into kinetic energy i.e., more the convective currents are intense and agitated more this the transformation will be completed near to the wall.

CONCLUSION

The thermal studies enabled us to highlight a difference in temperature between the stored liquid mass and evaporative surface.

In the liquid mass of the continuous fluctuations of temperature, at frequency and amplitude variables, confirm the distribution of the heat conveyed by the currents of convection.

The superheated state is the normal one whereby surface vaporisation takes place and the convective processes at the liquid vapour interface are independent of the depth the cryostat.

The evaporative mass flux through the surface is directly correlated with the degree of superheat.

The theoretical study shows that the problem of natural convection with imposed heat flux remains unexplored.

In natural convection, it is impossible to solve the momentum and energy equations independently of one another because the velocity, u, driven by buoyancy, is reflected in the momentum equation.

The thicknesses of interfacial and wall boundary layer decrease with the heat flow absorbed by the stored liquid where the effect of the surface tension as driving of instability can be under consideration on the level of the interface.

The behaviour's difference between the two modes can be explained by the fact that thermal energy will be converted into kinetic energy and this transformation is larger in the turbulent mode.

NOMENCLATURE

L : Height of the liquid bath (m)
L_v : Latent heat of vaporization (kJ kg^{-1})
T : Temperature (K)
T_b : Bulk temperature of the liquid mass (K)
Ts : Liquid surface temperature (K)
Z : Thickness of the mixture zone (m)
c_p : Specific heat (kJ $kg^{-1}.K^{-1}$)
g : Acceleration of gravity (m sec^{-2})
k : Thermal conductivity (W $m^{-1}.K^{-1}$)
$\dot{m}$: Evaporation mass flow rate (kg/sec/m^2)
u : Boundary layer velocity in x-direction (m sec^{-1})
v : Boundary layer velocity in y-direction (m sec^{-1})
x : Vertical coordinate (m)
y : Horizontal coordinate (m)
β : Thermal coefficient of expansion (K^{-1})
δ : Thickness of the parietal boundary layer (m)
δ_L : Thickness of the interfacial boundary layer (m)
δ_t : Thickness of the interfacial thermal boundary layer (m)
φ_L : Density heat flux of the liquid mass (W m^{-2})
φ_P : Density heat flux in the wall (W m^{-2})
ρ : Fluid density (kg m^{-3})
ν : Kinematic viscosity (m^2 sec^{-1})
μ : Dynamic viscosity (kg/m/sec)
ω : Modulate velocity in the boundary layer (m sec^{-1})

REFERENCES

Belmedani, M., 1994. Thèse de Magister. Conception d'un cryostat de mesure et application à l'étude du phénomène d'instabilité des liquides cryogéniques en stockage, U.S.T.H.B., Alger.

Belmedani, M., A. Belgacem and R. Rebiai, 2007. Modélisation de l'écoulement convectif dans le GNL en stockage. 1° CIGP'07, Béjaia, Algérie 28-30 octobre 2007.

Boukeffa, D., M. Boumaza, M.X. François and S. Pellerin, 2001. Experimental and numerical analysis of heat losses in liquid nitrogen cryostat. Applied Therm. Eng., 21: 967-975.

Catton, I., 1978. Natural convection in enclosures. In: Proceedings 6th Internatioal Heat Transfer Conference, 6: 13.

Chandrasekhar, S., 1962. Hydrodynamic and Hydromagnetic Stability. Oxford University Clarendon Press.

De Lorenzo, T., 2002. Convection naturelle transitoire le long d'une surface verticale soumise à une densité de flux périodique. C.R. Mecanique, 330: 181-184.

Eckert, E.R.G. and T.W. Jackson, 1950. Analysis of turbulent free convection boundary layer on flat plate. NACA Report, Vol. 1015.

Evans, L.B., R.C. Reid and E.M. Drake, 1968. Transient natural convection in vertical cylinder. AIChE. J., 14 (2): 251-259.

Incropera, F.P. and D.P. De Witt, 2002. Fundamentals of Heat and Mass Transfer. 5th Edn. Wiley and Sons.

Kadja, M. and R. Hacene, 1999. Simulation numérique de la convection naturelle d'un liquide soumis à des conditions pariétales variables. Int. J. Therm. Sci., 38: 348-354.

Kakaç, S. and Y. Yener, 1995. Convective Heat Transfer. 2nd Edn. Boca Raton, CRC Press.

Khelifi Touhami, M.S., A. Benbrik, D. Lemonnier and D. Blay, 2005. Convection naturelle en régime laminaire dans une cavité cylindrique. Application au stockage de GNL. 12° JITh, Tanger, Maroc du 15 du 17 Novembre 2005, 227-230.

Khemis, O., M. Boumaza , M. Ait Ali and M.X. François, 2003. Experimental analysis of heat transfers in cryogenic tank without lateral insulation. Applied Therm. Eng. J., 23: 2107-2117.

Khemis, O., R. Bessaïh, M. Ait Ali and M.X. François, 2004. Measurement of heat transfers in cryogenic tank with several configurations. Applied Therm. Eng., 24: 2233-2241.

Lienhard, J.H. IV and J.H.V. Lienhard, 2005. Heat Transfer Textbook. Cambridge MA., 3rd Edn. Phlogiston Press.

Ostrach, S., 1988. Natural convection in enclosures. J. Heat Trans.-T. ASME., 110: 1175.

Papanicolaou, E. and V. Belessiotis, 2002. Transient natural convection in a cylindrical enclosure at high Rayleigh numbers. Int. J. Heat Mass Transfer, 45: 1425-1444.

Polidori, G., C. Popa and T.H. Mai, 2003. Transient flow rate behaviour in an external natural convection boundary layer. Mech. Res. Commun., 30: 615-621.

Rashed, A.S. and M.M. Kassem, 2007. Group analyses for natural convection from a vertical plate. J. Comp. Applied Math. Article (In Press).

Rebiai, R., C. Beduz and R.G. Scurlock, 1984. Thermal overfill and the surface vaporisation of cryogenic liquids under storage conditions. Adv. Cryo. Eng., 29: 795-803.

Rebiai, R., 1985. Ph.D Thesis. The solubility of water in cryogenic liquids and related effects. Southampton University.

Taine, J. and J. Petit, 1989. Transferts Thermiques. mécanique des fluides anisothermes, Dunod.